Conformational Transition of Poly(γ-benzyl-L-glutamate)-Poly(ethylene glycol) Block Copolymers in Bulk

Young-Wook Choi, Youngmi Park, Jaebum Choo,† Chong Su Cho,‡ and Daewon Sohn*

*Department of Chemistry, Hanyang University, Seoul 133-791, Korea. *E-mail: dsohn@hanyang.ac.kr*
†Department of Applied Chemistry, Hanyang University, Ansan 426-791, Korea
‡School of Agricultural Biotechnology, Seoul National University, Seoul 151-921, Korea
Received February 3, 2007

The bulk properties of poly(γ-benzyl-L-glutamate)-poly(ethylene glycol), PBLG-PEO, diblock copolymer were investigated. The helical transition from 7/2 to 13/5 for pure PBLG was at 120 °C while those of GE-1 and GE-2, which contain flexible PEO block 40 wt% and 60 wt% respectively, were shown at 135 °C on DSC experiments. FT-IR and XRD experiments were shown that the diblock copolymers maintained their α-helical structure in the temperature range between 25 °C and 175 °C. Increasing relative size of coil part resulted in the increase of intermolecular packing distances. Due to well-maintained helical structure, lyotropic LC phases were observed for the PBLG-PEO block copolymer by the polarized optical microscope (POM). Especially, GE-3 copolymer, which has 12.5 wt% PEO contents, showed the smectic C phase. The competition of favorable aggregation energy between rod-rod and coil-coil, and unfavorable aggregation energy of rod-coil give rise to change the supramolecular structure in mixed solvent.

Key Words : Block copolymer, Rod-coil copolymer, PBLG-PEO, Smectic C phase, Aggregation energy

Introduction

Macromolecules with well defined structures on the nanometer scale are perfect candidates for self-assembled materials and nanometer scale devices.[1] Recent works from several researchers have shown that the amphiphilic diblock copolymers are able to form well-defined ordered and disordered nanostructures.[2-4] Rod-coil molecules consisting of a rigid rod block and a flexible coil block are a block copolymer with a unique microstructural organization held together by noncovalent forces including hydrophobic and hydrophilic effects, electrostatic interaction and hydrogen bonding.[5-8] The well-known polypeptide, poly(γ-benzyl-L-glutamate) (PBLG), has inter- and intramolecular hydrogen bonds that stabilize the secondary structures and shows mesoscopic liquid crystal order because of its good solubility and rodlike structure. Due to the lyotropic and thermotropic phase transition of PBLG, there are a lot of studies to make well-organized supra-molecular structures.[9,10] Since Robinson discovered the lyotropic liquid crystalline phase of PBLG, many research groups have studied rod-ordering theory of the liquid crystalline state with PBLG LC model.[11-14] It is, however, hard to observe smectic phase in PBLG solution predicted by Flory,[15] due to the polydispersity of synthetic PBLG. To understand the absence of smectic phase in lyotropic PBLG solution, Tirrell group adopt the bio-synthetic method to prepare the monodispersed PBLG.[9] With this PBLG, they showed PBLG smectic phase prepared in solution and were maintained its structure in transferred film. Other distinct characteristics of PBLG are biostability and biocompatibility. Poly(L-amino acid)s present outstanding physicochemical and biological properties, including mechanical properties, nontoxcity, and lower antigenicity.[16] But they are so brittle that it is difficult to apply them to living organs without combing them with other techniques.[17] PEO, that is one of the best-studied in a wide range of chemical and biomedical field, is quite safe in living body. So many research groups with PBLG-PEO copolymer have been investigated to find good mechanical properties or to control with nanometer length scale.[18-21] In previous works, from circular dichroism measurements in ethylene dichloride solution, we found that the polypeptide block exists in the α-helical conformation and adopts right-handed helix as in PBLG homopolymer.[22] However, the helix sense of PBLG in the copolymer nanoparticles prepared from organic solvent depends on the PEO contents in the copolymer and the nature of solvent. Through Langmuir-Blodgette experiment, monolayer microstructure of PBLG-PEO block copolymer depends on the free energy changes between rod and coil blocks.[23] Herein, the conformational changes as different ratios of rigid rod and flexible coil were discussed in solid state using DSC, temperature-controlled FT-IR and XRD. And PBLG-PEO liquid crystalline state was investigated through polarized optical microscopy in $CHCl_3$/TFA which is known as a solution mixture kept α-helical structure of PBLG rod part.

Experimental Section

Materials. γ-benzyl-L-glutamate *N*-carboxyanhydride (BLG-NCA) was prepared according to the method described by Goodman *et al*.[24] The PBLG-PEO diblock copolymers were prepared by the ring-opening polymerization of BLG-NCA initiated with primary-amine-terminated PEO in methylene dichloride. PBLG-PEO block copolymer composition was estimated from the peak intensity of the NMR signal of

Table 1. The molecular weight and the monomer ratio of GE-1, GE-2, GE-3, and GE-4

Polymer	Mw (Dalton)	Monomer unit ratio	fPBLG
GE-1	103,700	60.5 : 39.5	0.60
GE-2	51,800	40.0 : 60.0	0.4
GE-3	20,400	12.5 : 78.5	0.12
GE-4	18,000	10 : 90	0.10

*PEO Mw 12,000, PBLG:PEO ratios are obtained by the relative integration ratio of NMR peaks, fPBLG=NPBLG monomer unit/(NPBLG monomer unit + NPEG monomer unit)

methylene protons of the PBLG block and the signal of the ethylene proton of the PEO block. Full assignment of this polymer was discussed in previous paper.[23] The ratios of PBLG:PEO copolymers and their codes are summarized in Table 1.

Differential Scanning Calorimetry. A Mettler Toledo Star DSC, capable of programmed cyclic temperature runs over the range −110-300 °C, was used. Samples were first heated to the melt state with a rate 10 °C/min and subsequently cooled to −30 °C with the same rate. The transition temperature and enthalpies were obtained in the second heating with the same rate.

Fourier Transform Infrared (FTIR) Spectroscopy. Absorbance-FTIR experiment was carried out with temperature-control accessory with Bio-Rad FTS-6000. The temperature was controlled from 25 °C to 125 °C and the spectrum was acquired with 2 nm resolution.

Polarized Optical Microscopy (POM) PBLG-PEO diblock copolymers are dissolved in the mixture solvent of chloroform ($CHCl_3$, 97%) and trifluoroacetic acid (TFA, 3%). These solutions, 1-3 mg/mL, were transferred to a flat glass capillary tube. The capillary tube was carefully flame-sealed. And the capillary tube was placed on the polarized optical microscopy (POM) and their phase change was observed. In solid phase, their image of GE-4 diblock copolymer was obtained by heating up to temperature corresponding to the melt state and subsequently cooling down to 25 °C through POM.

X-ray Scattering. Wide-angle measurement was performed by a Shimadzu XRD-6000. The Cu Kα radiation, wavelength 1.54 Å, was used from a Siemens generator operating at 35 kV and 30 mA. Measurements were made in the 2θ range from 0.1° to 40° in steps of 0.1°.

Molecular Dynamics Simulation. Atomistic molecular dynamics simulation using the MMFF force field has been employed to investigate structural effect between PBLG and PEO. Two step calculations were executed to generate PBLG-PEO copolymer model. First, single PEO polymer molecule having molecular weight of 12,000 was constructed to have the TTG (trans-trans-gauche) configuration. The generated structure was minimized and then carried out simulation for 200ps at 25 °C using the MMFF forcefield.[25] For 200ps simulation, all hydrogen atoms were fixed using the SHAKE algorithm[26] and time step of 1 fs was employed with a velocity verlet integration method. The abbreviated PBLG-PEO copolymer model was constructed to save the computing time. The PEO segment was kept 40 wt% ratio as followed real weight. PBLG conformation was constructed with α-helix and the entangled PEO coordinate came from simulation structure. The generated structure was minimized and then carried out simulation for 200ps at 25 °C with fixed PBLG part and all hydrogen. The interaction energy was calculated by varying the distance with two copolymer molecules.

Results and Discussion

Thermal Behaviors. The DSC results of PBLG and GE series are shown in Figure 1. There are considerable difference between the first heating run and the second run for the samples. Typically, PBLG homo-polymer (Mw: 60,000 g/mol) has a great transformation at around 120 °C. In the first heating, the endothermic peak near 120 °C is known as reflection of the first-order transformation between two helical conformations from 7/2 to an 13/5 α-helical conformation.[27] This transformation is irreversible process in homo-peptide so that in the second heating, the endothermic peak near 120 °C is not shown.

In the GE copolymers, depending on the peptide volume fraction, GE-1 and GE-2 show one transition peak but GE-3 two transition peaks. The peak at 120 °C comes from typical PEG melting state. The endothermic peak about helical transition is 120 °C in PBLG homo-polymer, and 135 °C in GE-1, GE-2, and GE-3. PEG has lower melting point than that of PBLG, so generally increasing the PEG volume fraction, the transition temperature has to be decreased. But DSC experiment shows opposite characteristics. Therefore, the PBLG part shows some characteristic figures on thermal behaviors until the monomer ratio of PEG is up to 88 wt% in block copolymers. The helical structure is a representative crystalline state of PEG. In the helical structure of PEG, the bonds of the backbone are arranged in a trans-trans-gauche

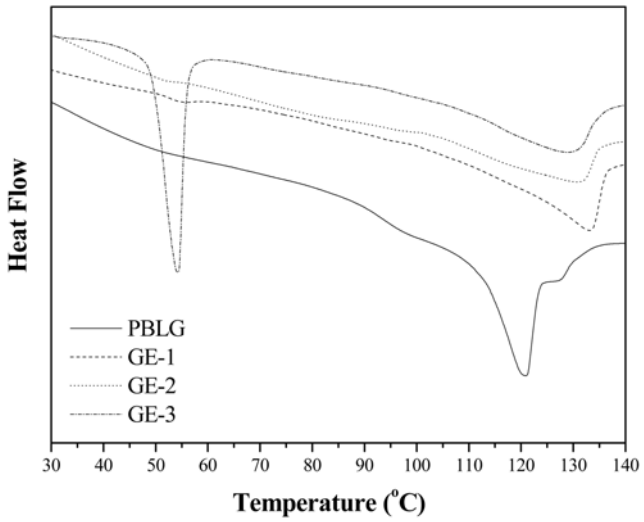

Figure 1. DSC heating traces (first heating cycle, 10 °C/min) for the PBLG (solid line), GE-1 (dashed line), GE-2 (dotted line), and GE-3 (dash dotted line).

(TTG) order, where the gauche angle is rotated uniformly with respect to the C-C-O plane over the length of the helix. It is called 7/2 helix of PEG crystal. PBLG also has the 7/2 helical conformation at low temperature helix, that is the reason why GE series have different DSC peaks with pure peptide bond. At high temperature, the melting part of PEG prevents PBLG aggregation from establishing tight 13/5 helical structure, so the higher temperature is needed.

The DSC experiments show that helical structure transition from 7/2 to 13/5 is affected by PEO contents. To confirm secondary structural transition on DSC experiments, FT-IR experiments are carried out. The characteristic peptide secondary structure can be confirmed by FT-IR spectrum. Amide I is the most intense absorption band in proteins and governed by the stretching vibrations of the C=O (70-85%) and C-N groups (10-20%). The absorption frequency is independent of the amino acid sequence, its hydrophilic or hydrophobic properties, and their charges. The frequencies of the main absorption bands from synthetic polypeptides adopting an antiparallel chain structure are at 1630 cm^{-1} while the absorption frequencies of α-helix are at 1650 cm^{-1}. The parallel β sheet structure that is not common in synthetic polypeptides leads to an amide I absorption near 1640 cm^{-1}.[28] Amide II derives mainly from in-plane N-H bending (40-60% of the potential energy). The rest of the potential energy arises from the C-N (18-40%) and the C-C (about 10%) stretching vibrations.[29] The frequencies of the main absorption bands from synthetic polypeptides adopting an antiparallel chain structure are at 1530 cm^{-1} while the absorption frequencies of α-helix are at 1550 cm^{-1}.

As shown Figure 2(a), main absorption peaks of Amide I at 1653 cm^{-1} and Amide II at 1543 cm^{-1} are appeared with PBLG homopolymer that keep the α-helix conformation. A small shoulder at 1630 cm^{-1} showed in PBLG homopolymer contains a little β-sheet conformation. In PBLG homopolymer, Amide I band is shown frequency change from 1653 cm^{-1} to 1655 cm^{-1} toward high frequency region, but Amide II band is shifted from 1543 cm^{-1} to 1539 cm^{-1} toward low frequency region on temperature-dependent FT-IR spectra. This peak band changes mean transition from 7/2 to 13/5 that is agreed with DSC experiments. While GE series contain PEO parts, the amide I peak mainly appears about 1651 cm^{-1} and amide II peak about 1545 cm^{-1} at low temperature. As increasing temperature, these peaks show the 13/5 helical conformation. FT-IR experiment clearly reveals that conformations of PBLG parts are affected by the PEG part. All GE series show 7/2 helical structure, while β-sheet structure just shows a little shoulder peak, and all 7/2 structures are transformed to 13/5 conformation at high temperature. In generally, 13/5 helical structure adopt the hexagonal packing with X-ray experiment. To study spacing effect of PEG parts, XRD experiments are executed. WAXD patterns of all GE series are shown in Figure 3.

The WAXS pattern of PBLG taken at room temperature shows the typical columnar hexagonal packing of α-helix. The first peak near 5° corresponds to intermolecular spacing of PBLG rod. The pitch of the helix generally observed between first peak and broad amorphous halo is not shown in the GE series. The broad amorphous halo between 10-20 ° indicates that there is a long amorphous side chain. These results are in agreement with the previous published X-ray study. The assignment is based on the (020) plane of the orthogonal unit cell with the β-conformation of peptide.[30] The WAXD patterns at 19° and 23° are characteristics of

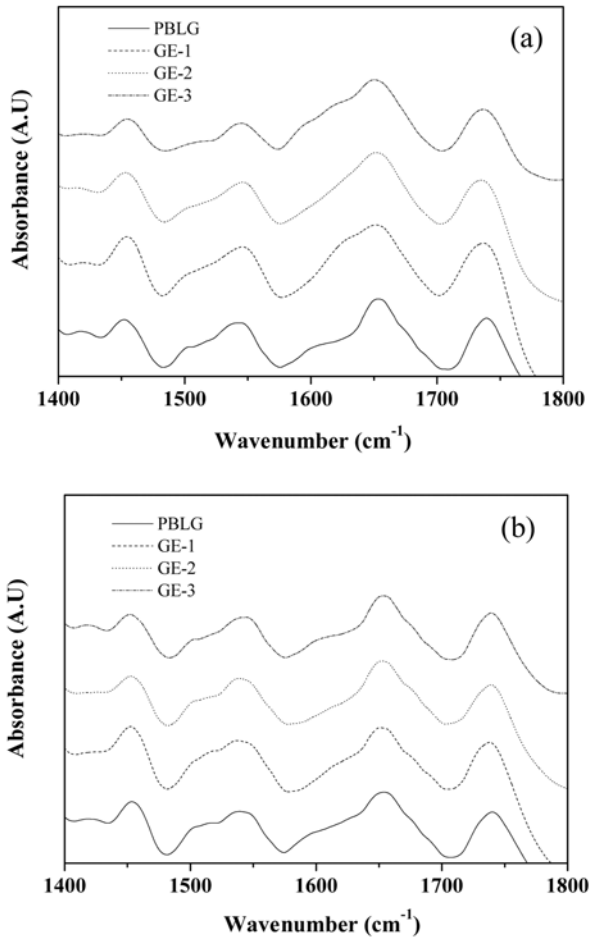

Figure 2. Temperature-dependent FT-IR spectra of PBLG and GE series (a) at 25 °C and (b) at 150 °C.

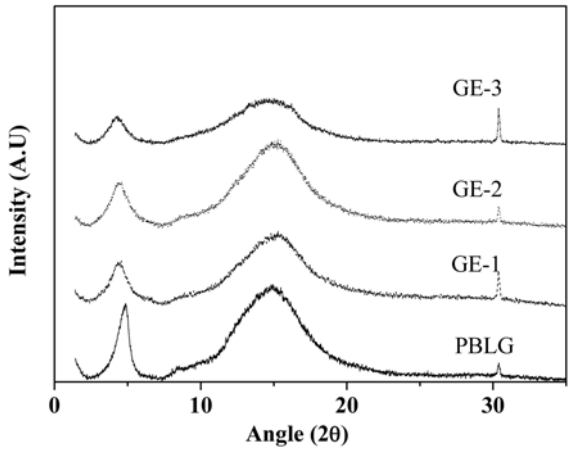

Figure 3. Wide angle X-ray diffraction patterns of GE series at 25 °C.

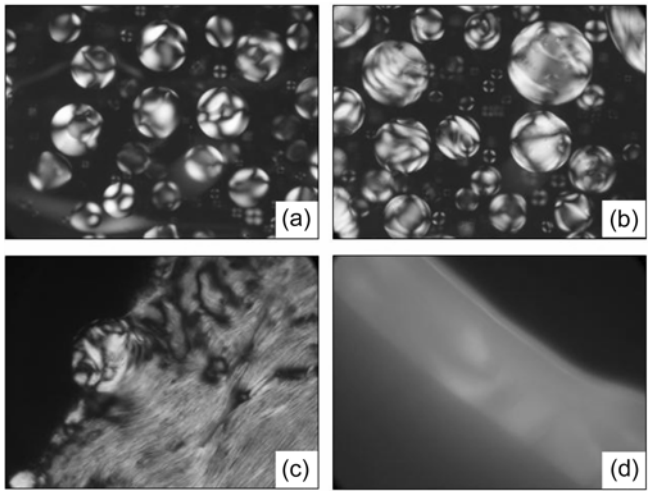

Figure 4. Polarized optical microscopy images taken in mixed solvent of chloroform ($CHCl_3$, 97%) and trifluoriacetic acid (TFA, 3%) at room temperature (a) PBLG, (b) GE-1, (c) GE-2, and (d) GE-3.

PEO crystals where the PEO chains form a 2/7 helix structure.[17] This means all GE series keep the α-helical conformation, and the contents of β-conformation increased PBLG parts are reduced because of repulsion between PEG and PBLG. The β-sheet conformation is also indicated by small shoulder peak in FT-IR spectra

Liquid Crystalline Image. The liquid crystalline properties of PBLG and PBLG-PEO diblock copolymers (GE series, GE-1, GE-2 and GE-3) are investigated in the mixed solvent of chloroform ($CHCl_3$, 97%) and trifluoroacetic acid (TFA, 3%). α-helical conformations of PBLG-rod are maintained in the solvent mixture, and addition of TFA, as reported, inhibits aggregation of PBLG in concentrated solutions while maintaining the PBLG-rod rigidity of the chain.[31] The lyotropic liquid crystalline (LC) image of PBLG (Mw 50,000 g/mol) with polarized optical microscopy (POM) is shown in Figure 4.

Lyotropic liquid crystalline polymer has its phase transition depending on both temperature and concentration. At low concentration, lyotropic LC phase could not be observed. As the concentration increases, birefringent LC phase (nematic phase) was appeared. Yu *et al.* reported that this nematic LC phase is caused by the polydispersity of synthetic PBLG.[9] They showed that monodisperse PBLG synthesized by biochemical method did not exhibit the nematic droplets in solution mixture ($CHCl_3$/TFA) but in some condition it showed fan-like texture, smectic phase, which could be characterized by orientation of molecules.

Figure 4(b), (c), and (d) show POM images of GE-1, GE-2 and GE-3 which indicate LC phase transition with different amorphous portion in the mixed solvent of $CHCl_3$ and TFA. The LC phase behaviors of PBLG-PEO diblock copolymers were different from that of conventional polydisperse PBLG homopolymer. For the GE-1 with gradually increased concentration, birefringent droplet LC phase is appeared like LC image of synthetic PBLG, but the image of GE-1 has more layered structure as shown in Figure 4(b). GE-2 shows a transition from the birefringent nematic phase to filament-like smectic C phase, as shown in Figure 4(c). The spaced lines are related to the pitch of the phase in filament-like smectic C phase. GE-3 with the short rod just shows a transition from isotropic phase to LC phase, as shown in Figure 4(d). A fingerprint texture of the cholesteric phase is generally observed with PBLG homopolymer, but filament-like smectic C phase has not been reported yet.

Table 2. The radius of gyration of GE-1, GE-2, and GE-3

	GE-1	GE-2	GE-3
R_g (Å)	15.27	14.73	15.77
STDEV	0.29	0.17	0.16

Table 3. The interaction energy between PBLG and PEO parts of GE-1, GE-2, and GE-3

	VDW	ELEC	Tot INTE
GE-1	−11.23	−6.94	−18.18
GE-2	−11.72	−3.44	−15.17
GE-3	−28.62	−10.06	−38.68

Molecular Dynamics Simulation. There are many theories of changing effect in molecular structure on the smectic C phase. The conclusions that can be drawn from early studies are as follows: 1) Smectic C phase is very dependent on the molecular structure of the constituent molecules, particularly on the chain length of terminal groups. 2) The phase is usually exhibited by compounds having approximately symmetrical molecular structures. 3) Terminal outboard dipole moments help to increase the chances that compounds exhibit a smectic C phase.

The molecular dynamics simulation is a useful tool to probe these explanations. The value of radius of gyration of GE series determined by the molecular dynamic simulation is given in Table 2. The radii of gyration is 15.27 Å for GE-1, 14.73 Å for GE-2, and 15.77 Å for GE-3, which means the dimension of PEO parts is not affected by the contents of PBLG.

Therefore, smectic C phase of GE-2 and GE-3 results from symmetrical structure between PBLG and PEO parts. The interaction energy is calculated to evaluate not only the effect of symmetrical structure but also the dipole moment of the each molecule. The calculation results are shown in Table 3.

Total interaction energy is 18.18 kcal/mol for GE-1, 15.27 kcal/mol for GE-2, and 38.68 kcal/mol for GE-3. GE-3 shows the highest interaction energy due to the electrostatic interaction. The electrostatic interaction plays a crucial role in stabilizing macromolecular conformations as well as mediating the interactions between macromolecules.

Therefore, smectic C phase of GE-3 can be explained because of good interaction between hydrophobic rod of PBLG that is approximately symmetrical and hydrophilic chain of PEO that has strong dipole moment. According to the Semenov and Vasilenco (SV) theory, the self-assembly of rod-coil copolymers is affected by cohesion and adhesion

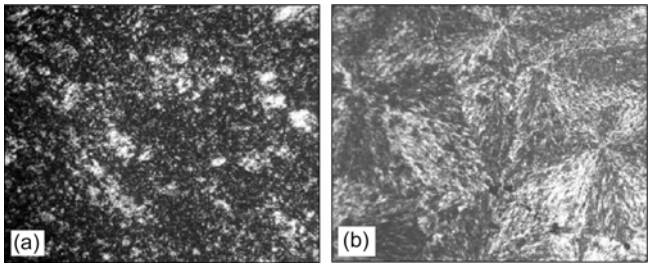

Figure 5. Polarized optical microscopy images of GE-4 (a) at PEO melting temperature of 65 °C, and (b) at crystalline temperature of 34 °C.

free energy.[32] The aggregation favorable cohesion free energy is consisted of the rod-rod interaction and coil-coil interaction energy. And the aggregation unfavorable adhesion free energy is consisted of the rod-coil interaction energy. In PBLG and GE-1 series has the bigger rod molecule so the cohesion energy is dominant, while GE-3 series has the bigger chain molecule so the adhesion energy is dominant.

The GE-4 comprised of almost PEO part does not characteristic figure in solution but shows spherulites. This result suggests PEO molecule has 7/2 zig-zag helical conformation. Figure 5 shows the polarized optical microscopic images of GE-4 (a) at PEO melting temperature of 65 °C, (b) at its crystalline temperature of 34 °C.

Conclusion

The rod-coil interaction of PBLG homopolymer and PBLG-PEO block-copolymer has been studied. High molecular weight of block copolymer, PBLG-PEO, makes to maintain α-helical structure regardless of PEG contents. The amide I peak in the FT-IR spectrum, however, is shifted toward lower frequency region because of the 7/2 helical structure of PEG crystalline state, and DSC transition peaks from 7/2 to 13/5 conformation are also shifted toward high temperature region. Although FT-IR spectra show a little shoulder peak representing β-sheet structure, β-sheet peak is not clearly observed in XRD experiments. While all molecules are typical hexagonal packing as result of XRD experiment, relative radius of gyration magnitude of PEG is enlarged by increasing the inter-molecular distance. The hexagonal packing is shown the lyotropic LC state in mixed solvent. Especially, GE-2 series show the smectic C phase which is not observed in polydispersed PBLG. The control of aggregation energy between cohesion free energy and adhesion free energy can be used to explain the formation of smectic C phase.

Acknowledgment. This work was supported by the research fund from the National R & D Project for Nano Science and Technology in Korea (KISTEP). DS thanks for the the ABRL program of KOSEF (grant #: R-14-2002-004-01002-0).

References

1. Yu, S. M.; Soto, C. M.; Tirrell, D. A. *J. Am. Chem. Soc* **2000**, *122*, 6552.
2. Chen, J. T.; Thomas, E. L.; Ober, C. K.; Mao, G. *Science* **1996**, *273*, 343.
3. Stupp, S. I. *Curr. Opin. Colloid Interface Sci.* **1998**, *3*, 20.
4. Gallot, B. *Prog. Polym. Sci.* **1996**, *21*, 1035.
5. Whitesides, G. M.; Mathias, J. P.; Seto, C. P. *Science* **1991**, *254*, 1312.
6. Muthukumar, M.; Ober, C. K.; Thomas, E. L. *Science* **1997**, *277*, 1225.
7. Foster, S.; Antonietti, M. *Adv. Mater.* **1998**, *10*, 195.
8. Israelachvili, J. N. *Intermolecular and Surface Forces;* Academic Press: London, 1992.
9. Yu, S. M.; Conticello, V. P.; Zhang, G.; Kayser, Ch.; Fournier, M. J.; Mason, T. L.; Tirrell, D. A. *Nature(London)* **1997**, *389*, 167.
10. He, S.-J.; Lee, C.; Gido, S. P.; Yu, S. M.; Tirrell, D. A. *Macromolecules* **1998**, *31*, 9387.
11. Robinson, C.; Ward, J. C. *Nature* **1957**, *180*, 1183.
12. Straley, J. P. *Mol. Cryst. Lig. Cryst.* **1973**, *22*, 333.
13. Horton, J. C.; Donald, A. M.; Hill, A. *Nature* **1990**, *346*, 44.
14. Wee, E. L.; Miller, W. G. *J. Phys. Chem.* **1971**, *75*, 1446.
15. Flory, P. J. *Proc. R. Soc. London, Ser. A* **1956**, *234*, 73.
16. Katchalski-Katzir, E. *Acta Biochim. Pol.* **1996**, *43*, 217.
17. Tanaka, S.; Ogura, A.; Kaneko, T.; Murata, Y.; Akashi, M. *Macromolecules* **2004**, *37*, 1370.
18. Nah, J.-W.; Jeong, Y.-I.; Cho, C.-S. *Bull. Korean Chem. Soc.* **2000**, *21*(4), 383.
19. Nah, J.-W.; Jeong, Y.-I.; Cho, C.-S. *Bull. Korean Chem. Soc.* **1998**, *19*(9), 962.
20. Kataoka, K.; Kwon, G. S.; Yokoyama, M.; Okano, T.; Sakurai, Y. Mccleland, C. P.; Batemen, R. L. *J. Controlled Release* **1993**, *24*, 119.
21. Kwon, G. S.; Naito, M.; Kataoka, K.; Yokoyama, N.; Sakurai, Y.; Okano, T. *Collids Surf. B* **1994**, *2*, 429.
22. Cho, C.-S.; Kobayshi, A.; Goto, M.; Akaike, T. *Thin Solid Films* **1995**, *264*, 82.
23. Park, Y.; Choi, Y.-W.; Park, S.; Cho, C.-S.; Falsoka, M. J.; Sohn, D. *J. Colliod and Interface Sci.* **2005**, *283*, 322.
24. Fuller, W. D.; Goodman, V. M. *Biopolymers* **1976**, *15*, 869.
25. Thomas, A.; Halgren, J. *J. Comput. Chem.* **1996**, *17*, 490.
26. Allinger, N. L.; Young, Y. H.; Lii, J.-H. *J. Am. Chem. Soc.* **1989**, *111*, 8551.
27. Lecommandoux, S.; Achard, M.-F.; Langenwalter, J. F.; Klok, H.-A. *Macromolecules* **2001**, *34*, 9100.
28. Miyazawa, T.; Blout, E. R. *J. Am. Chem. Soc.* **1961**, *83*, 712.
29. Kubelka, J.; Keiderling, T. A. *J. Am. Chem. Soc.* **2001**, *123*, 6142.
30. Floudas, G.; Papadopoulos, P.; Klok, H.-A.; Vendermeulen, G. W. M.; Rodriguez-Hernandez, J. *Macromolecules* **2003**, *36*, 3673.
31. Duke, R. W.; Du Pre, D. B.; Hines, W. A.; Samulski, E. T. *J. Am. Chem. Soc.* **1976**, *98*, 3094.
32. Semenov, A. N.; Vasilenko, S. V. *Sov. Phys.-JEPT (Engl. Transl.)* **1986**, *63*, 70.